Hybrid structural control based on the combination of tuned mass damper and variable slip-force level damper

P. XIANG & A. NISHITANI
Department of Architecture, Waseda University, Japan

SUMMARY:
This paper presents a hybrid control strategy based on the combination of tuned mass damper (TMD) and variable slip-force level damper (VSFLD). VSFLD used in this paper, is a semi-actively controlled damper which provides an elastic-perfectly plastic hysteresis with variable slip-force levels, and can be controlled so as to maintain a ductility factor of two responding to harmonic excitations. The ductility factor of two is firstly demonstrated to be the optimum value for an elastic-perfectly plastic hysteresis in mitigating the maximum relative displacement amplitude of steady-state resonant vibrations. Then the hybrid control strategy is applied to a base-isolated structure, and an optimization method is adopted to design TMD in the system. Based on the numerically simulated results, the hybrid control strategy is demonstrated to be effective for both harmonic excitations and real non-stationary seismic excitations and can effectively protect base-isolated structures from low-frequency resonance induced by long period ground motions.

Keywords: Hybrid control, TMD, variable slip-force level damper, optimization method

1. INSTRUCTIONS

Tuned mass damper (TMD) is one of the simplest and most reliable structural control devices in terms of reducing the resonant vibration of a primary structure. Variable slip-force level damper (VSFLD) used in this paper, of which the concept was already published by Nishitani et al. (2003), is a semi-actively controlled damper which provides an elastic-perfectly plastic hysteresis with variable slip-force levels. It can be controlled so as to maintain a ductility factor of two responding to harmonic excitations. The ductility factor of two is the optimum value in mitigating the relative displacement amplitude of steady-state resonant vibrations. By hybrid-combining TMD and VSFLD, enhancement of response control performance to different kinds of seismic excitations can be achieved.

First of all, it is theoretically demonstrated that, with the ductility factor of two, an elastic-perfectly plastic hysteresis would be the most effective in mitigating the steady-state resonant vibration to harmonic excitations. Secondly, an optimization method is presented to determine the optimum parameters of TMD. Then, the hybrid control strategy is applied to a base-isolated structure, and the dynamic iterative equation of the hybrid-controlled nonlinear system is derived. Through numerical simulations of such constructed hybrid-controlled system to different types of seismic excitations, the effectiveness of the hybrid control strategy is demonstrated by comparing with the un-control, passive control based on only TMD and semi-active control based on only VSFLD.

2. VARIABLE SLIP-FORCE LEVEL DAMPER

VSFLD is a semi-actively controlled damper which provides an elastic-perfectively plastic hysteresis with variable slip-force levels. Its concept has been proposed by Nishitani et al. (2000, 2003). It is controlled so as to maintain a ductility factor of two responding to harmonic excitations. It has been demonstrated that, with the ductility factor of two, an elastic-perfectly plastic hysteresis would be the most effective in mitigating steady-state vibrations to harmonic excitations (Nishitani et al. 2009).

Herein, however, the different way is employed for demonstrating that a ductility factor of two is the optimum value for mitigating the relative displacement amplitude of steady-state resonant vibrations.

The hysteresis loop of an elastic-perfectly plastic damper is shown in Fig. 2.1. k_d represents the stiffness of the damper, k_{seq} denotes the required equivalent linear stiffness of the system, and α is the ratio of k_d to k_{seq}. x_y and μ are the elastic limit deformation and ductility factor, respectively. Then the equivalent linear stiffness k_{deq} and equivalent viscous damping coefficient c_{deq} of the damper can be obtained as

$$k_{deq} = \frac{k_d}{\mu} = \frac{\alpha k_{seq}}{\mu} \ , \quad c_{deq} = \frac{4(\mu-1)\alpha k_{seq}}{\pi \mu^2 \omega} \tag{2.1}$$

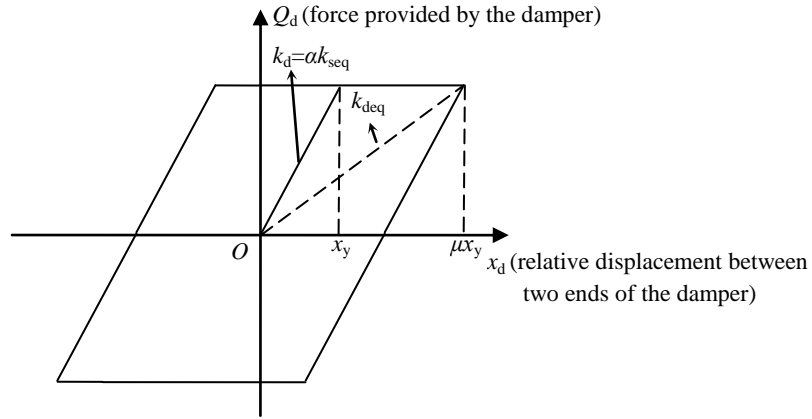where ω is circular frequencies of harmonic excitations.

Figure 2.1 Elastic-perfectly plastic hysteresis loop

Under the condition that the total equivalent linear stiffness, k_{seq}, of the structure incorporating with the damper is unchanged, the stiffness of the structure, k_s, and the equivalent damping ratio, ζ_{eq}, of the whole system can be obtained as Eqns. 2.2 and 2.3, respectively.

$$k_s = k_{seq} - k_{deq} = \frac{\mu - \alpha}{\mu} k_{seq} \tag{2.2}$$

$$\zeta_{eq} = \sqrt{\frac{\mu - \alpha}{\mu}} \zeta_s + \frac{2(\mu-1)\alpha \omega_{seq}}{\pi \mu^2 \omega} \tag{2.3}$$

where ζ_s and ω_{seq} denote the damping ratio of the structure and equivalent linear natural circular frequency of the whole system, respectively, and ζ_s is around in the range of 0.01~0.02 for most building structures.

The relative displacement amplitude x_m of the steady-state resonant vibration for the damper attached structure is

$$x_m = \frac{m_s A_g / (2k_{seq})}{\zeta_{eqr}} = \frac{m_s A_g / (2k_{seq})}{\sqrt{\frac{\mu - \alpha}{\mu}} \zeta_s + \frac{2(\mu-1)\alpha \omega_{seq}}{\pi \mu^2 \omega_{seq}}} = \frac{m_s A_g / (2k_{seq})}{\sqrt{\frac{\mu - \alpha}{\mu}} \zeta_s + \frac{2(\mu-1)\alpha}{\pi \mu^2}} \tag{2.4}$$

where m_s denotes the mass of the structure, ζ_{eqr} represents the equivalent damping ratio of the combined system of the structure and VSFLD for the case of resonance, and A_g is the amplitude of a harmonic excitation.

It can be found that x_m is minimum when ζ_{eqr} is maximum. In other words, the minimum value of x_m can be obtained when the first and second order derivatives of ζ_{eqr} with respect to μ are equal to zero and negative, respectively. The equation of the first order derivative of ζ_{eqr} is

$$(16 - \pi^2\zeta_s^2)\mu^3 - 16(4+\alpha)\mu^2 + 64(1+\alpha)\mu - 64\alpha = 0 \tag{2.5}$$

The coefficient $\pi^2\zeta_s^2$ in Eqn. 2.5 can be neglected compared with the coefficient 16, thus the following formulation can be obtained.

$$(\mu\text{-}2)^2(\mu-\alpha) = 0 \tag{2.6}$$

It can be found from Eqn. 2.6 that two is the optimum value of the ductility factor μ; otherwise k_s will be zero. On the other hand, it can be easily proved that the second order derivative of ζ_{eqr} with respect to μ is negative when μ equals two. Therefore, when the ductility factor of the elastic-perfectly plastic damper is equal to two, the relative displacement amplitude of the steady-state resonant vibration can be maximally mitigated. In the case of steady-state harmonic oscillations, zero displacement occurs when velocity reaches its peak value. Therefore, VSFLD is designed so as to slip when the peak velocity is reached, and then the ductility factor of two will be automatically satisfied.

The behavior of the hysteresis depicted in Fig. 2.1 could be compared with that of a visco-elastic damper (VED). Fig. 2.2 shows the hysteresis loops for VSFLD and its corresponding VED when responding to a harmonic excitation with increasing amplitude. It can be found that the resulting relative displacements are identical to each other for the two hystereses, while the maximum force required by the equivalent VED is 19% larger than VSFLD. In addition, there are several disadvantages for VED as follows: properties are temperature-dependent; the design is in general complex and cumbersome; and visco-elastic materials are possibly de-bonding and tearing. In consideration of these properties for VED, VSFLD could be idealistic alternatives of VED.
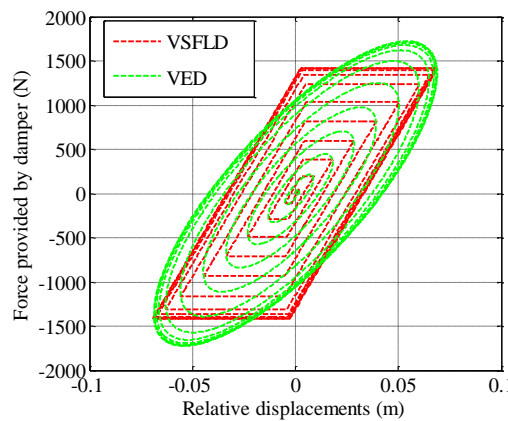

Figure 2.2 Hysteresis loops for VSFLD and equivalent VED

3. DESIGN OF TMD

In this section, the optimum design of TMD for a structural system integrating VSFLD is discussed. A

hybrid-controlled system combining TMD and VSFLD as shown schematically in Fig. 3.1 is considered. VSFLD is installed between the primary structure and ground. The symbols m, k and c denote the mass, stiffness and damping coefficient, respectively. The subscript s represents structure, and T represents TMD.

If the structure is lightly-damped, such as damping ratio of 0.01~0.02, those damping ratios have practically very little influence on the optimum parameters of a linear TMD (Ankireddi and Yang, 1996; Rüdinger, 2006). Accordingly, it is reasonable to neglect the damping ratio in determining the optimum parameters of TMD based on the fixed points theory (Den Hartog, 1956). Even for those moderately-damped structures to which the fixed points theory can be no longer applied, the quasi-fixed points theory has been employed by some researchers (Tsai et al. 1993; Asami et al. 1995; Ghosh et al. 2007). It is derived under the condition that the assumption used in the fixed points theory also approximately holds when TMD is attached to a moderately damped structure.
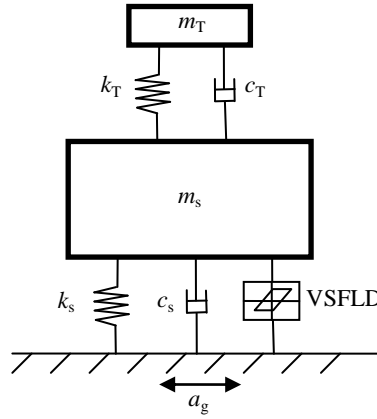

Figure 3.1 Analytic model of hybrid-controlled system

Numerical searching procedures can be used for the optimal design of TMDs corresponding to each specific situation. In this study, gradient-based optimization analysis method is employed. The optimization problem can be formulated to search the optimal set of the design variables over an admissible domain so as to minimize the objective function set (the maximum absolute value of frequency transfer functions in this study). Herein the design variables are the frequency ratio of TMD to primary structure, υ, and the damping ratio of TMD, ζ_T. It should be noted that gradient-based method requires a set of initial values with respect to the design variables and the method efficiency and accuracy are quite sensitive to the setting of these initial values. This numerical method is classified into the local optimum method category rather than the global optimum method category. To derive a global optimization result, a number of sets of initial values are given in terms of random numbers (e.g., using *rand* function in MATLAB), and then the global optimum parameters υ_{opt} and ζ_{Topt} are searched. It is not time-consuming to carry out the above analysis.

In designing TMD for the hybrid-controlled system, the equivalent damping ratio of the combination of the primary structure and VSFLD for the case of resonance, ζ_{eqr}, is regarded as the damping ratio of the total structure.

The circular frequency and damping coefficient of TMD can be obtained as

$$\omega_T = \upsilon_{opt}\omega_{seq}, \quad c_T = 2m_T\zeta_{Topt}\omega_T \tag{3.1}$$

where

$$m_T = \eta m_s \tag{3.2}$$

The frequency transfer functions of the equivalent linear primary structure from ground harmonic acceleration input to absolute acceleration response (denoted as $|H_{As}|$) are shown in Fig. 3.2 (a) and (b), respectively, with parameters of μ and α. The dashed lines in the figures represent the cases without TMD, while the solid lines correspond to the cases with TMD. In Fig. 3.2(a), the optimum ductility factor is found two, which is consistent with the result discussed in the Section 2.1. On the other hand, Fig. 3.2 (b) demonstrates the effectiveness of the employed hybrid control strategy, presenting the fact that the maximum amplitudes of the frequency transfer functions are largely mitigated. With larger stiffness of VSFLD, the larger mitigation can be achieved, whereas TMD is less effective.
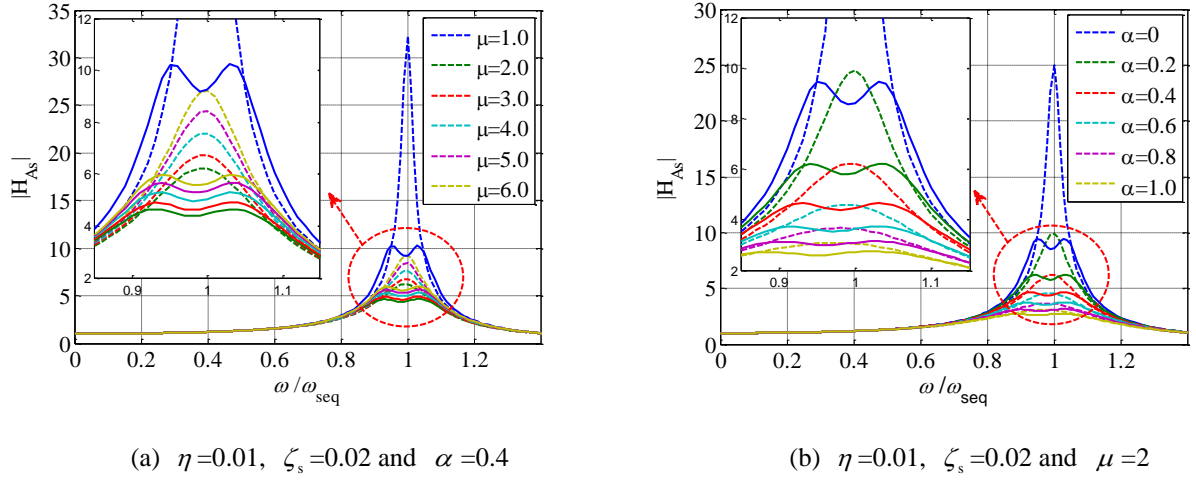

(a) $\eta = 0.01$, $\zeta_s = 0.02$ and $\alpha = 0.4$

(b) $\eta = 0.01$, $\zeta_s = 0.02$ and $\mu = 2$

Figure 3.2 Frequency transfer functions of absolute accelerations for primary structure

4. ANALYSIS OF HYBRID-CONTROLLED BASE-ISOLATED STRUCTURE

4.1. Analytic model and method

In the following, the hybrid structural control strategy is applied to a base-isolated structure. The structural model is schematically illustrated in Fig. 4.1.
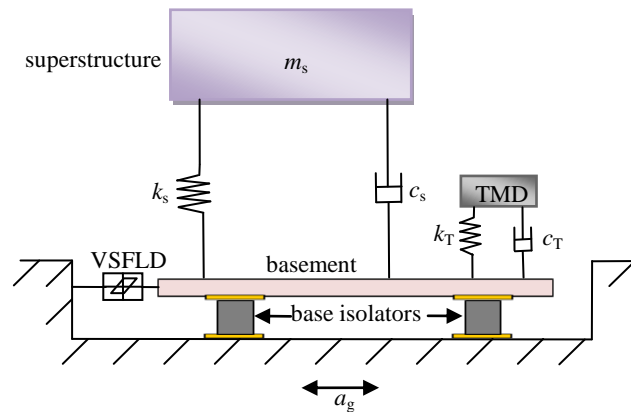

Figure 4.1 Hybrid-controlled base-isolated structural analytic model

VSFLD is treated as a non-linear element in the following time domain discussion, although the effect of VSFLD was approximately estimated by the equivalent linearization method in the frequency domain discussion.

With a_g representing the ground acceleration, the equation of motion for the 3DOF system shown in Fig. 4.1 can be written as

$$\mathbf{M}\ddot{\mathbf{x}} + \mathbf{C}\dot{\mathbf{x}} + \mathbf{K}\mathbf{x} + \mathbf{r}_1 Q_\text{d} = -\mathbf{M}\mathbf{r}_2 a_\text{g} \tag{4.1}$$

where $\mathbf{M} = \begin{bmatrix} m_\text{b} & 0 & 0 \\ 0 & m_\text{s} & 0 \\ 0 & 0 & m_\text{T} \end{bmatrix}$, $\mathbf{C} = \begin{bmatrix} c_\text{b} + c_\text{s} + c_\text{T} & -c_\text{s} & -c_\text{T} \\ -c_\text{s} & c_\text{s} & 0 \\ -c_\text{T} & 0 & c_\text{T} \end{bmatrix}$, $\mathbf{K} = \begin{bmatrix} k_\text{b} + k_\text{s} + k_\text{T} & -k_\text{s} & -k_\text{T} \\ -k_\text{s} & k_\text{s} & 0 \\ -k_\text{T} & 0 & k_\text{T} \end{bmatrix}$,

$\mathbf{r}_1 = \begin{Bmatrix} 1 \\ 0 \\ 0 \end{Bmatrix}$, $\mathbf{r}_2 = \begin{Bmatrix} 1 \\ 1 \\ 1 \end{Bmatrix}$, $\ddot{\mathbf{x}} = \begin{Bmatrix} \ddot{x}_\text{b} \\ \ddot{x}_\text{s} \\ \ddot{x}_\text{T} \end{Bmatrix}$, $\dot{\mathbf{x}} = \begin{Bmatrix} \dot{x}_\text{b} \\ \dot{x}_\text{s} \\ \dot{x}_\text{T} \end{Bmatrix}$ and $\mathbf{x} = \begin{Bmatrix} x_\text{b} \\ x_\text{s} \\ x_\text{T} \end{Bmatrix}$.

Solving Eqn. 4.1 based on the Newmark-β method, the dynamic iterative equation expressed by the variable $\mathbf{x}$ can be obtained as

$$\mathbf{x}_{n+1} = \left[\frac{1}{\beta(\Delta t)^2}\mathbf{M} + \mathbf{K} + \frac{\gamma}{\beta \Delta t}\mathbf{C} \right]^{-1} \cdot$$

$$\left\{ \left[\left(\frac{1}{2\beta} - 1 \right)\mathbf{M} - \left(1 - \frac{\gamma}{2\beta} \right)\Delta t \mathbf{C} \right]\ddot{\mathbf{x}}_n + \left[\frac{1}{\beta \Delta t}\mathbf{M} - \left(1 - \frac{\gamma}{\beta} \right)\mathbf{C} \right]\dot{\mathbf{x}}_n \right. \tag{4.2}$$

$$\left. + \left[\frac{1}{\beta(\Delta t)^2}\mathbf{M} + \frac{\gamma}{\beta \Delta t}\mathbf{C} \right]\mathbf{x}_n - \mathbf{M}\mathbf{r}_2 a_{\text{g},n+1} - \mathbf{r}_1 Q_{\text{d},n+1} \right\}$$

where, $\mathbf{x}_n$, $\dot{\mathbf{x}}_n$ and $\ddot{\mathbf{x}}_n$ are displacement, velocity and acceleration vectors at the time instant nT (T is the sampling time); and $\mathbf{x}_{n+1}$, $a_{\text{g},n+1}$ and $Q_{\text{d},n+1}$ are the displacement vector, ground acceleration scalar and VSFLD force scalar at the time instant $(n+1)T$, respectively. $\gamma = 0.5$ and $\beta = 0.25$ are employed. $\mathbf{x}_{n+1}$ can be solved iteratively during the time period $nT \sim (n+1)T$ from Eqn. 4.2, and then $\dot{\mathbf{x}}_{n+1}$ and $\ddot{\mathbf{x}}_{n+1}$ can be obtained by the following formulations:

$$\dot{\mathbf{x}}_{n+1} = \frac{\gamma}{\beta \Delta t}(\mathbf{x}_{n+1} - \mathbf{x}_n) + \left(1 - \frac{\gamma}{\beta} \right)\dot{\mathbf{x}}_n + \left(1 - \frac{\gamma}{2\beta} \right)\Delta t \ddot{\mathbf{x}}_n \tag{4.3}$$

$$\ddot{\mathbf{x}}_{n+1} = -\mathbf{M}^{-1}(\mathbf{C}\dot{\mathbf{x}}_{n+1} + \mathbf{K}\mathbf{x}_{n+1} + \mathbf{r}_1 Q_{\text{d},n+1}) - \mathbf{r}_2 a_{\text{g},n+1} \tag{4.4}$$

Subsequently, $\mathbf{x}$, $\dot{\mathbf{x}}$ and $\ddot{\mathbf{x}}$ at the next time step can be obtained from Eqns. 4.2-4.4.

4.2. Numerical simulations

With the computer program written based on the above method, the hybrid controlled system is analyzed in different excitation situations. The mass, natural period and damping ratio of the superstructure are 1.0×10^6 kg, 1.0s and 0.02, respectively. The mass of the basement is 5.0×10^4 kg, the natural period and viscous damping ratio of the base isolators are assumed to be 2.5s and 0.10, respectively, and α is set to be 0.6. The mass ratio of TMD to the primary structure is 0.05. The frequency and damping ratios of TMD are determined by the optimization method presented in

Section 3 with the objective function set as the maximum absolute value of the frequency transfer function for the deformation of base isolators; they are υ_{opt} =0.91 and ζ_{Topt} =0.13 for the passive control; and υ_{opt} =0.87 and ζ_{Topt} =0.15 corresponding to the hybrid control. The sampling time is set to be 0.01s in all calculations.

4.2.1. Harmonic resonant excitation
The case in which the frequency of a harmonic excitation is equal to the fundamental natural frequency of the base-isolated structure is considered. In Fig. 4.2 two different hysteresis loops of VSFLD are presented. The green and red solid lines, respectively, correspond to the case of only VSFLD (referred to as "semi-active" in the figure) and the case of the combination of TMD and VSFLD (referred to as "hybrid" in the figure). It is evident from the figure that the algorithm of VSFLD exhibits satisfactory hysteresis in both cases when the base-isolated structural system is subjected to harmonic excitations.

The response time histories (deformations of the base isolators, absolute accelerations of the basement, relative displacements and absolute accelerations of the superstructure) are shown in Fig. 4.3. In the figure, the blue dashed, black dashed, green solid and red solid lines correspond to the un-controlled, passive-controlled (only with TMD), semi-active-controlled (only with VSFLD), and hybrid-controlled (with both TMD and VSFLD) responses, respectively. For the purpose of making quantity evaluation of the resulting control effects of these control schemes, Fig.4.4 gives the response ratios of the three control schemes to the un-controlled case with respect to the maximum deformation of base isolators (Max.d_b), maximum and root mean square values of absolute acceleration of the superstructure (Max.a_s and RMS.a_s). It can be seen from the figure that, by incorporating both TMD and VSFLD into the system, all the responses are mitigated. Among the schemes, the hybrid control achieves the best control effect. Compared to the responses of the un-controlled case, i.e. simple base-isolated system, the responses are reduced by 36~40% for the passive control with only TMD; they are reduced by 36~46% for the semi-active control with only VSFLD; and they are reduced by 50~58% for the hybrid control with both TMD and VSFLD.
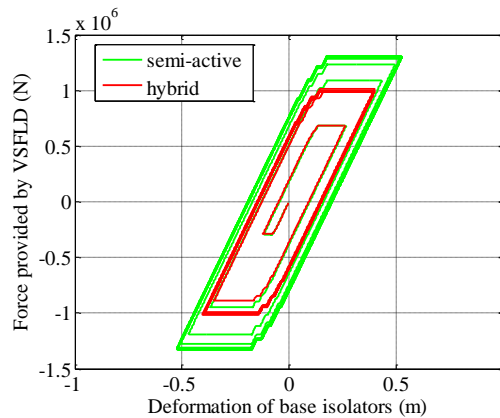

Figure 4.2 Hysteresis loops of VSFLD

4.2.2. Earthquake excitations
The effect of the hybrid control strategy is investigated by using four un-scaled actually-measured earthquake records: the 1940 Imperial Valley (El Centro Array 6, NS component, referred to as El Centro in the following), the 1995 Kobe (JMA, NS component), the 1999 Chi-chi (TCU068, EW component) and the 2011 Tohoku (TKY007, EW component). These seismic records are chosen as representatives of distinct classes of earthquakes (Hisada 2004; Takewaki *et al*. 2011). Fig. 4.5 shows the hysteresis loops of VSFLD for the case of the four different ground motions. It can be seen from the figure that VSFLD exhibits favorable hystereses even in responding to non-harmonic or random excitations.
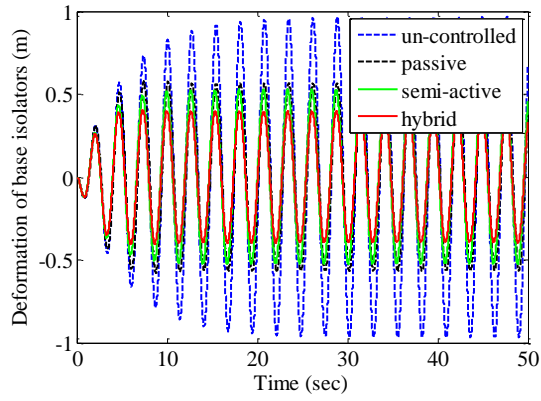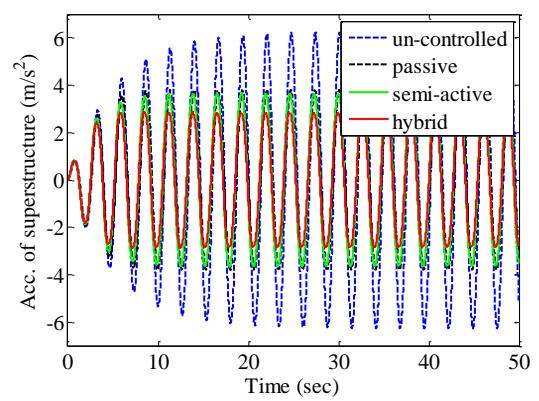
(a) Base isolator deformation
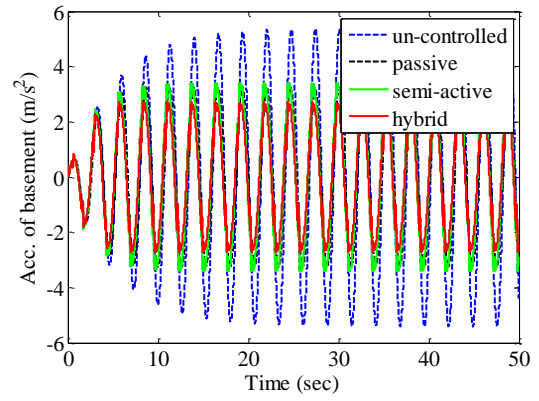
(b) Basement acceleration
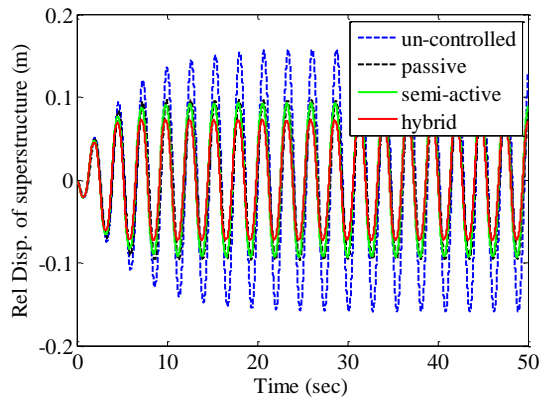
(c) Superstructure displacement relative to basement

(d) Superstructure acceleration
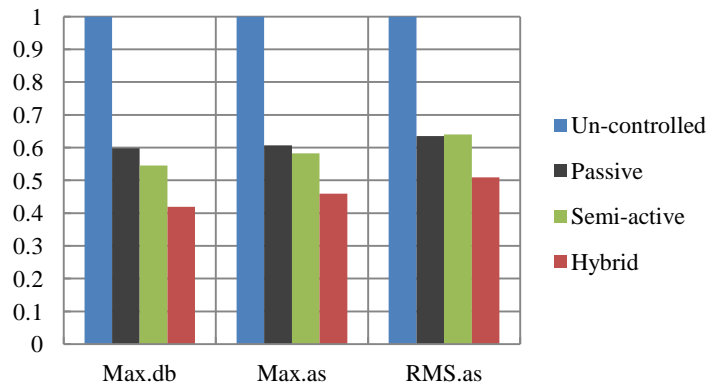
Figure 4.3 Time histories of responses

Figure 4.4 Response ratios of different control strategies

Fig. 4.6 gives the response ratios for the four earthquakes. It can be seen from Fig. 4.6 that, the hybrid control strategy in general achieves the best control performance. It is found from Fig. 4.6 (a) that, by the hybrid control, the reductions of Max.d_b are 15~20% for El Centro and Kobe, which are mainly comprised of short-period components; while 30~35% for Chi-chi and Tohoku which contain fairly large long-period components. From Fig. 4.6 (b) and (c), it can be seen that, by the hybrid control, Max.a_s and RMS.a_s can be mitigated by 25% and 32% at most, respectively.
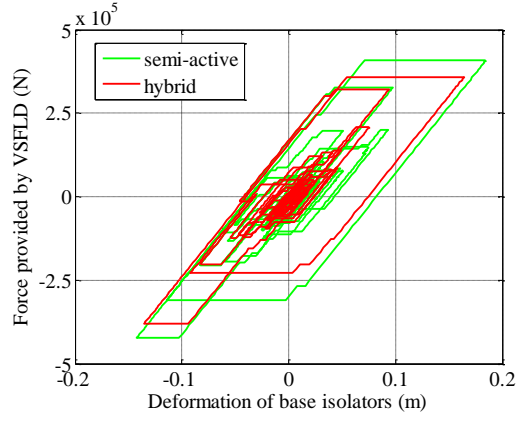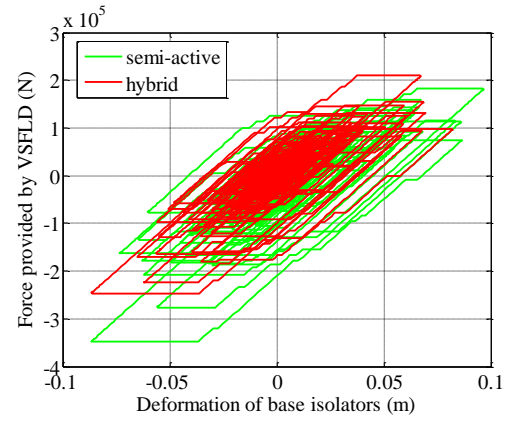
(a) El Centro
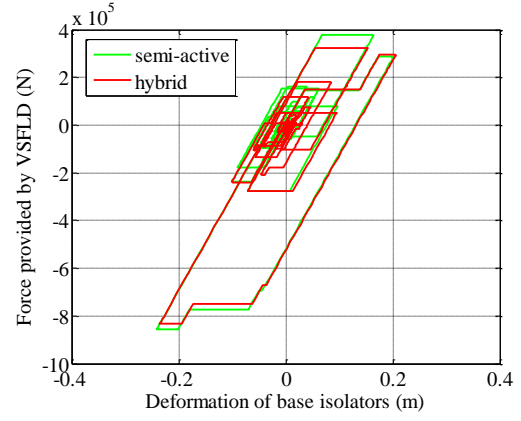
(b) Kobe
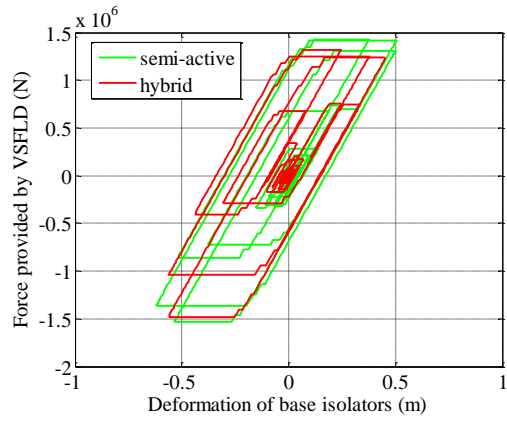
(c) Chi-chi

(d) Tohoku

Figure 4.5 Hysteresis loops of VSFLD

(a) Max.d_b

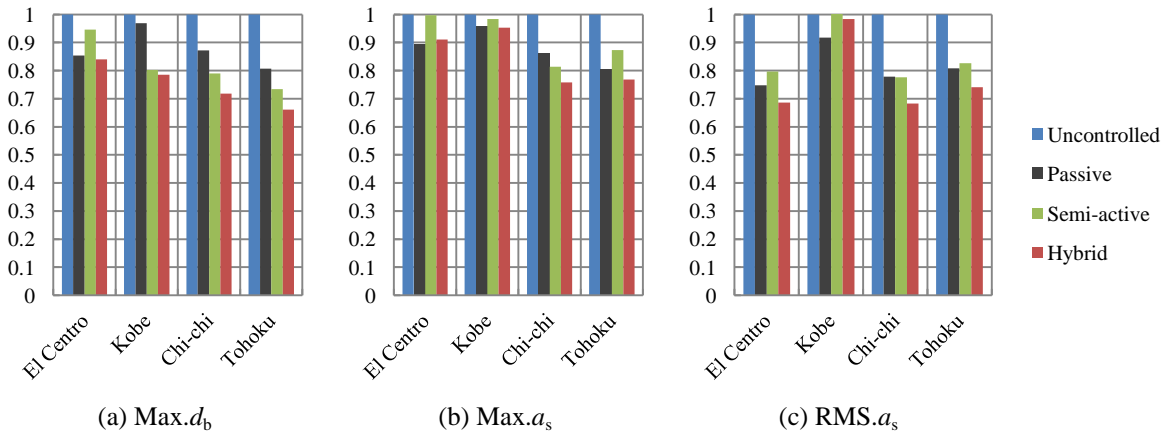(b) Max.a_s

(c) RMS.a_s

Figure 4.6 Response ratios of different control strategies

5. CONCLUSIONS

This paper presents a hybrid control strategy based on the combination of TMD and VSFLD. It is theoretically demonstrated that, with a ductility factor of two, an elastic-perfectly plastic hysteresis would be the most effective in mitigating the steady-state resonant vibrations. The hybrid control strategy is then applied to a base-isolated structure. An optimization method for designing the

parameters of TMD in the hybrid-controlled system is presented, and the dynamic iterative equation of the nonlinear system is also presented. Through the numerical simulations of the hybrid-controlled system to different types of ground excitations, the performance of the hybrid control strategy is demonstrated to be superior compared with TMD based passive control and VSFLD based semi-active control, especially for protecting the base-isolated structure from low-frequency resonance induced by long period ground motions.

REFERENCES

Ankireddi, S. and Yang, T.Y. (1996). Simple ATMD control methodology for tall buildings subject to wind loads. *Journal of Structural Engineering* **122:1**, 83-91.

Asami, T. and Hosokawa, Y. (1995). Approximate expression for design of optimal dynamic absorbers attached to damped linear systems. *Journal of the Japan Society of Mechanical Engineers* **61:583**, 915-921. (in Japanese)

Den Hartog, J.P. (1956). *Mechanical vibrations*, McGraw–Hill, New York.

Ghosh, A. and Basu, B. (2007). A closed-form optimal tuning criterion for TMD in damped structures. *Structural Control and Health Monitoring* **14**, 681-692.

Hisada, Y. (2004). Strong ground motion in near source area and earthquake damage. *Proceedings of Architectural Institute of Japan*. (in Japanese)

Nishitani, A., Nitta, Y., Itoh, A. and Ikeda, Y. (2000). Semiactive variable-friction damper control with simple algorithms. *Proceedings of the 2000 American Control Conference*. **Vol 1:** 503-507.

Nishitani, A., Nitta, Y. and Ikeda, Y. (2003). Semiactive Structural-Control Based on Variable Slip-Force Level Damper. *Journal of Structural Engineering* **129:7**, 933-940.

Nishitani, A., Nitta, Y. and Wakahara, C. (2009). Artificial nonlinearity in structural control: Its original concept survey and significance in semiacctive control scheme. *Structural Control and Health Monitoring* **16**, 17-31.

Rüdinger, F. (2006). Optimal vibration absorber with nonlinear viscous power law damping and White Noise excitation. *Journal of Engineering Mechanics* **132:1**, 46-53.

Takewaki, I., Murakami, S., Fujita, K., Yoshitomi, S. and Tsuji, M. (2011). The 2011 off the Pacific coast of Tohoku earthquake and response of high-rise buildings under long-period ground motions. *Soil Dynamics and Earthquake Engineering* **31:11**, 1511-1528.

Tsai, H.C. and Lin, G.C. (1993). Optimum tuned-mass dampers for minimizing steady-state response of support-excited and damped structures. *Earthquake Engineering and Structural Dynamics* **22**, 957-973.